J Appl Electrochem (2011) 41:1–6
DOI 10.1007/s10800-010-0201-z

ORIGINAL PAPER

Highly active carbon-supported PdNi catalyst for formic acid electrooxidation

Yanwei Gao · Gang Wang · Bing Wu · Chao Deng · Ying Gao

Received: 11 January 2010 / Accepted: 5 September 2010 / Published online: 19 September 2010

Abstract A new carbon-supported PdNi (PdNi/C) catalyst is prepared by a simple simultaneous reduction reaction with sodium borohydride in glycol solution. The results show that the performance of PdNi/C catalyst for formic acid oxidation is greatly improved compared with that of Pd/C. X-ray diffraction (XRD) results show that Ni exists in the catalyst both as NiO and as PdNi alloy. The value of the apparent activation energy shows that the activity of formic acid oxidation on the PdNi/C is more sensitive to temperature compared with Pd/C.

Keywords Formic acid · Nickel · Palladium · Electrooxidation · Electrocatalysis

1 Introduction

Recently, the electrochemical oxidation of formic acid has been attracting increasing attention [1–6] because the direct formic acid fuel cell (DFAFC) has some advantages over the direct methanol fuel cell [7, 8]. For example, formic acid is non-toxic and nonflammable. Formic acid has low crossover effect through the Nafion membrane because of the anodic repulsion between the Nafion membrane and the partially dissociated form of formic acid [9, 10]. Another advantage is that highly concentrated formic acid can be used in DFAFC and can work well, while the highest concentration of methanol in DMFC is only about 2 M [11]. Thus, the power density of DFAFC can be higher than that of DMFC, though formic acid has a lower energy density than methanol (about one-third that of methanol). Initially, Pt-based catalysts were used for formic acid electrooxidation [12–15]; however, these electrocatalysts were easily poisoned by the CO-like intermediates formed in the formic acid oxidation reaction [16]. Recent research works have found that metal Pd was more active than Pt for formic acid electrooxidation [17–20]. Further investigations have demonstrated that Pd catalyst has its drawbacks as an anodic catalyst. One of the disadvantages of Pd as an anodic catalyst is its instability. The oxidation current greatly decreases over a longer process of the oxidation of formic acid on a Pd catalyst [21]. It was found that Pd catalyst initially shows high activity for formic acid oxidation, but the steady state activities are higher on PdPt than on Pd. It was reported that the catalytic activity and stability of Pd were increased by addition of another precious metal into the catalyst, such as Au [22], Pt [23] or Ir [24]. Non-noble metals such as Pb [25], Sn [22, 26], Co [27, 28] and boron [29] have also been used as promoters for formic acid catalytic electrooxidation. However, the performances of Pd catalysts need further improvement. Liu et al. recently reported that carbon-supported PdNi/C has higher electrocatalytic activity and lower onset potential for methanol oxidation than does a Pd/C catalyst [30]. In this study, carbon-supported PdNi catalysts were synthesized by chemical reduction with $NaBH_4$ with the expectation to enhance the activity and stability for the oxidation of formic acid. The physicochemical properties and electrochemical activities of the PdNi/C catalyst for formic acid oxidation in acidic media were investigated.

Y. Gao · G. Wang · B. Wu · C. Deng · Y. Gao (✉)
College of Chemistry and Chemical Engineering, Harbin Normal University, Harbin 150025, China
e-mail: yinggao99@126.com

2 Experimental

The preparation of carbon-supported PdNi/C catalysts can be briefly described as follows: 10 mL ethylene alcohol and 0.04 g of carbon black were mixed and ultrasonicated for 1 h at room temperature, followed by adding 5.0 mL $PdCl_2$ (3.508 g L^{-1} $PdCl_2$) and 1.7 mL $NiCl_2$ solution (4.530 g L^{-1} $NiCl_2{\cdot}6H_2O$) drop by drop within 15 min. After 2 h, the pH of the suspension was adjusted to 8, and an excess amount of $NaBH_4$ was added with stirring for 1.5 h. Finally, the slurry was filtered and dried under vacuum at 100 °C for 10 h. The catalyst was designated as PdNi/C, and the Pd:Ni atomic ratio was 3:1. The Pd/C catalyst was prepared similar to PdNi/C, except with no nickel chloride addition in the process.

The preparations of Pd/C and PdNi/C catalyst electrodes were as follows: A fixed amount of catalyst was mixed with 5% Nafion solution, 20% PTFE and ethanol and was ultrasonicated for 5 min. The obtained slurry was spread on a carbon paper and dried at room temperature. The Pd loading of the electrode was 1 mg cm^{-2}.

The electrochemical measurements were carried out with a CHI650A electrochemical analyzer and a conventional three-electrode electrochemical cell. The working electrodes were the Pd/C and PdNi/C catalyst electrode prepared above. Ag/AgCl in saturated KCl solution and a coiled Pt wire were used as the reference and the counter electrode, respectively. All potentials are quoted with respect to the Ag/AgCl electrode. Nitrogen gas (99.999%) was bubbled into the solution for 10 min to remove O_2 dissolved in the solution prior to the electrochemical measurements.

The composition of catalysts was determined using an energy dispersive spectrometer (EDS, S-4800, Hitachi, Japan). The X-ray diffraction (XRD) analyses of the catalysts were carried out with an X-ray diffractometer (Rigaku D/Max-IIIA) using a Cu K_α source operated at 40 keV, with tube current at 150 mA. Transmission electron microscopy (TEM) was performed with a Tecnais G2 Twins.

3 Results and discussion

The XRD patterns for catalysts are shown in Fig. 1. The first diffraction peak at $2\theta = 25°$ originates from Vulcan XC-72 carbon supported for the catalysts. The 2θ values of the other four peaks at Pd/C and PdNi/C are reflections of the face-centered cubic crystal lattice of the Pd(111), Pd(200) and Pd(220) crystal faces at the patterns of Pd/C and PdNi/C. However, the 2θ value of the characteristic peaks for the PdNi/C catalyst shifted to high 2θ values compared with those for Pd/C. This indicates that the Ni

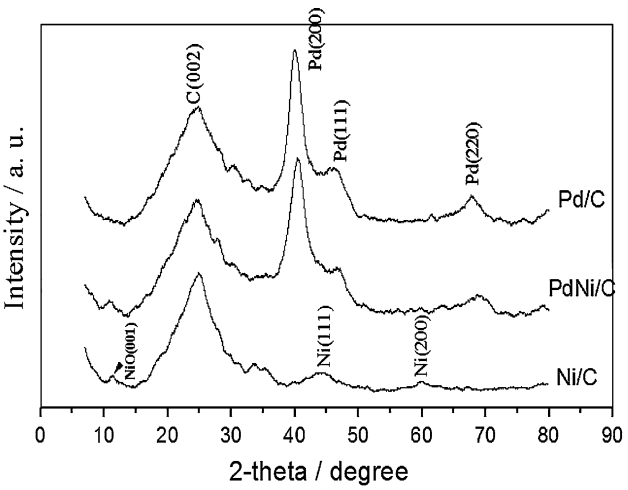

Fig. 1 XRD patterns of Pd/C, PdNi/C and Ni/C catalysts

atom entered into the Pd lattice and that an alloy of Pd and Ni was formed to some extent. Comparing the pattern of PdNi/C and Ni/C in Fig. 1, no diffraction peaks of Ni were found in the pattern of PdNi/C, except for NiO(001). This means that Ni exists in the catalyst both as NiO and PdNi alloy, which can be concluded from the lower lattice parameter. The lattice parameters for PdNi/C and Pd/C were evaluated from the angular position of the (220) reflection peak maxima by using Eq. 1

$$a = \frac{2^{1/2}\lambda_{K\alpha}}{\sin\theta_{\max}}, \tag{1}$$

where a is the lattice parameter (nm), $\lambda_{K\alpha}$ is the wavelength of X-rays used (0.154056 nm) and $\theta_{\max}$ is the Bragg angle at the peak maximum. The average particle size is estimated by using the Scherrer equation:

$$d = \frac{0.9\lambda_{K\alpha}}{B_{2\theta}\sin\theta_{\max}}, \tag{2}$$

where d is the mean particle size and $B_{2\theta}$ is the width (in rad) of the peak at the half-height. The calculated lattice parameter, the average particle size and the composition of the catalysts are listed in Table 1. Higher angle and lower lattice parameter indicate the formation of alloy due to the replacement of some Pd atoms in the Pd crystal structure by some smaller Ni atoms. The average metal particle size in the PdNi/C catalyst is smaller than that in the Pd/C catalyst (Table 1). The TEM images and the particle size

Table 1 The atomic ratio, composition, average particle size and lattice parameters of the prepared catalysts

Sample	Atomic ratio Pd:Ni	2θ (°) Pd(220)	a (nm)	d (nm)
Pd/C	1:0	67.9	0.390	3.2
PdNi/C	3.2:1	69.1	0.384	2.9

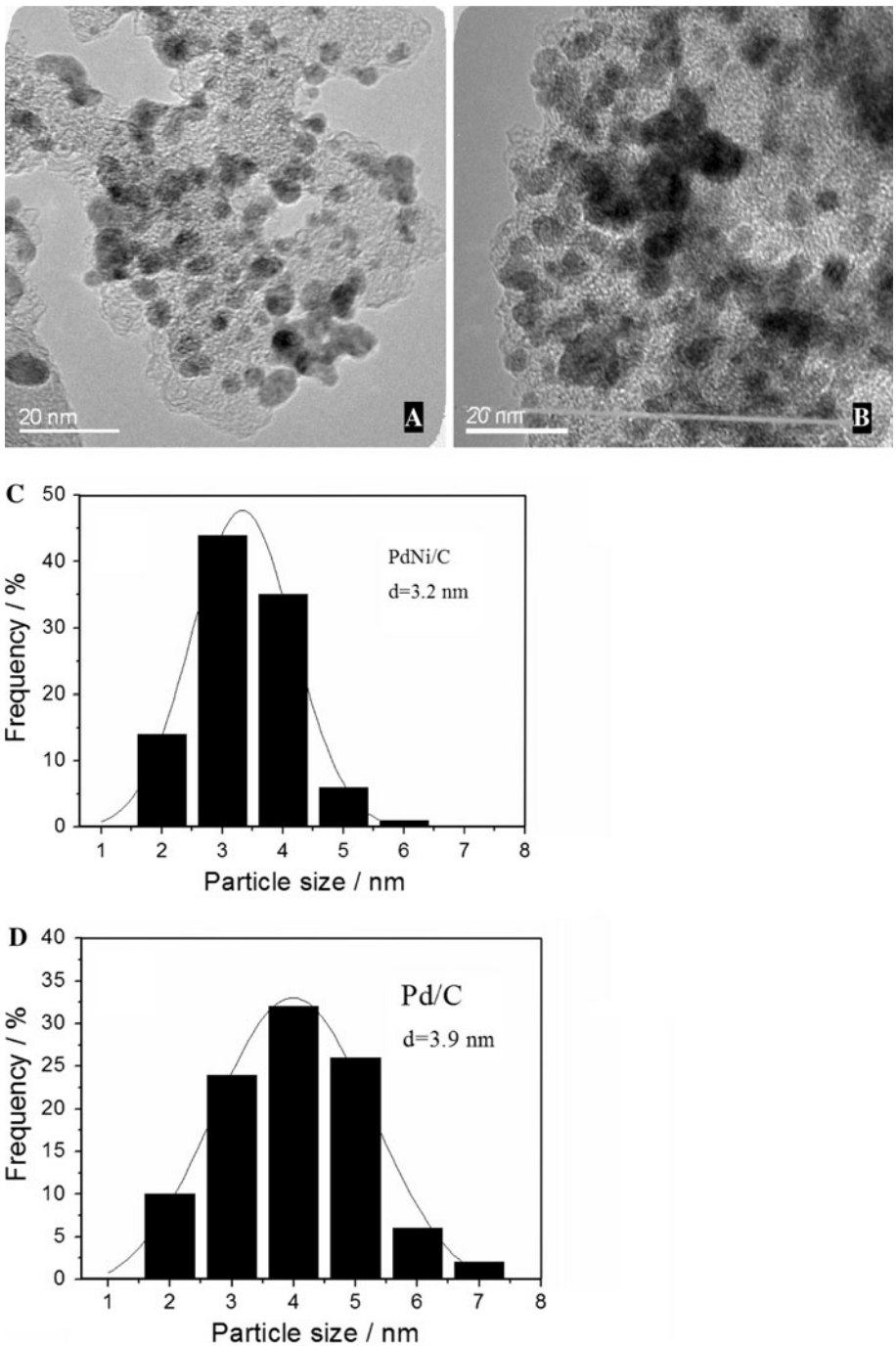

Fig. 2 TEM images (**A**, **B**) and their corresponding particle size distribution histograms (**C**, **D**) of PdNi/C and Pd/C catalysts

distributions of Pd/C and PdNi/C catalysts are shown in Fig. 2. From Fig. 2A and B, it can be seen that the metal particles are more uniform on PdNi/C than on Pd/C, and some Pd nanoparticles are agglomerated in Pd/C catalyst (Fig. 2B). This result indicates that adding Ni may help the dispersion of the Pd particles. The mean diameters of metal particles of PdNi/C and Pd/C catalysts are 3.2 and 3.9 nm, respectively (Fig. 2C, D). The particle diameters obtained from XRD measurement is basically consistent to that obtained from the TEM measurement.

Figure 3 shows the EDS spectrum of the PdNi/C catalyst. It can be obtained from Fig. 3 that the atomic ratio of Pd and Ni in the catalyst is 3.2:1, indicating that Pd and Ni contents in the PdNi/C catalysts were about the same as those in the initial mixtures in the solution. The small oxygen peak showed in Fig. 3 means that some Ni atoms exist as nickel oxide. This result is consistent with the XRD.

Figure 4 is the cyclic voltammograms of Pd/C and PdNi/C catalyst electrodes in 0.5 M H_2SO_4 solution at

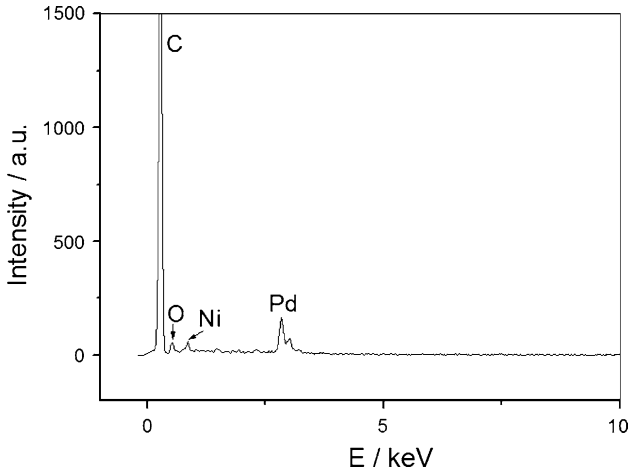

Fig. 3 The EDS spectrum of the PdNi/C catalyst

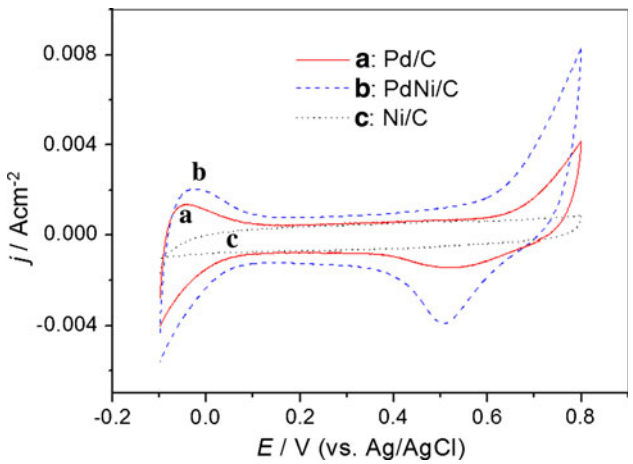

Fig. 4 Cyclic voltammograms of 0.5 M H_2SO_4 solution at (*a*) Pd/C, (*b*) PdNi/C and (*c*) Ni/C catalyst electrodes at 25 °C. Scan rate: 10 mV s^{-1}

25 °C. It can be observed from Fig. 4 that the peak in the hydrogen adsorption–desorption region on PdNi/C is higher than that on Pd/C. This means that the electrochemical surface area at PdNi/C is larger than that on Pd/C. The charge/discharge current of the double layer at the PdNi/C catalyst electrode is also larger than that at Pd/C because the PdNi/C possesses smaller average size of the metal particles, leading to largest surface area. However, no peak of hydrogen adsorption and desorption was found at Ni/C, illustrating that Ni alone is not active for hydrogen adsorption–desorption.

Figure 5 shows the linear sweeping voltammograms of 1.0 M HCOOH in 0.5 M H_2SO_4 solution at Pd/C and PdNi/C catalyst electrodes at 25 °C. No anodic peak is evident at the Ni/C catalyst electrode (Fig. 5, curve c), indicating that the Ni/C catalyst has no electrocatalytic activity for the oxidation of formic acid. The potential of the main anodic peak of formic acid at PdNi/C catalyst electrode is 0.05 V,

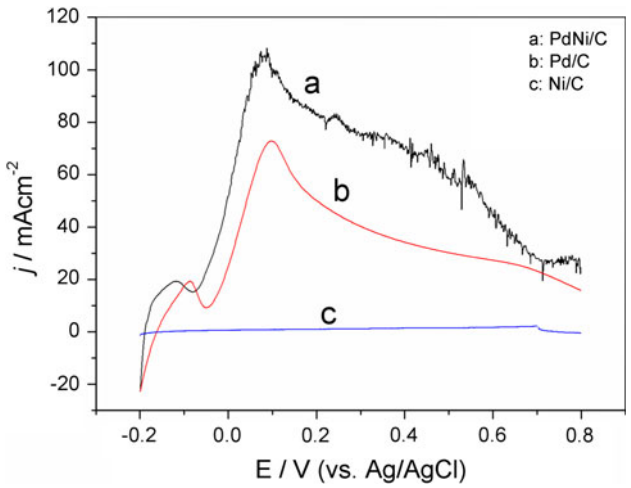

Fig. 5 Linear sweep voltammograms on (*a*) PdNi/C, (*b*) PdNi/C and (*c*) Ni/C in 1.0 M HCOOH + 0.5 M H_2SO_4 at 25 °C. Scan rate: 10 mV s^{-1}

which is about 40 mV more negative than that at Pd/C catalyst electrode. The current densities of the main peak at PdNi/C and Pd/C catalyst electrodes were 105.1 and 72.9 mA cm^{-2}, respectively. The onset potential of formic acid oxidation at PdNi/C catalyst electrode is 30 mV more negative than that at Pd/C catalyst electrode. The above results illustrate that the electrocatalytic activity of PdNi/C catalyst electrode for formic oxidation is better than that of Pd/C catalyst electrode. Therefore, Ni can largely promote the electrocatalytic activity of Pd/C catalyst for formic acid oxidation. The reason for the promotion effect may be due to that Ni can contribute to the adsorption of oxygen-containing species, which is conducive to the oxidation of formic acid [30] and a change in electronic properties of Pd [31]. In addition, it should be mentioned that the curve at PdNi/C catalyst electrode in Fig. 5 is not smooth because a large amount of CO_2, the product of formic acid oxidation, escapes from the electrode surface.

The temperature dependence of formic acid oxidation at PdNi/C catalyst electrode in the temperature range of 20–60 °C was further investigated (Fig. 6). At the very low scan rate (2 mV s^{-1}), two anodic peaks of formic acid oxidation at about 0.05 and 0.65 V can be clearly observed. According to the reports, the anodic peak at the more negative potential (0.05 V) is attributed to the direct pathway for formic acid oxidation and the anodic peak at the more positive potential (0.65 V) is attributed to the CO pathway. First, it can be observed from Fig. 6 that the peak currents increase with increasing temperature, illustrating that the rate of formic acid oxidation at PdNi/C catalyst electrode increases with increasing the temperature at the range of 20–60 °C. Secondly, the increase rate of the peak current at about 0.65 V with increasing temperature is larger than that at 0.05 V. Thirdly, the peak at about 0.05 V

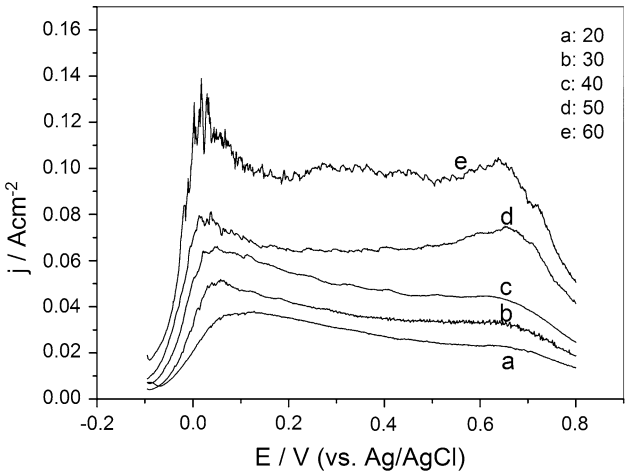

Fig. 6 Linear sweep voltammograms for 1.0 M HCOOH in 0.5 M H_2SO_4 on a PdNi/C electrode at different temperatures. Scan rate: 2 mV s^{-1}

is shifted to the negative potential with increasing the temperature, while the peak position at about 0.065 V is not basically shift with increasing the temperature. Above results illustrate that the temperature effect on formic acid oxidation reaction through the direct pathway is different from that through the CO pathway. It may be related to the activation energy of two formic acid oxidation reactions.

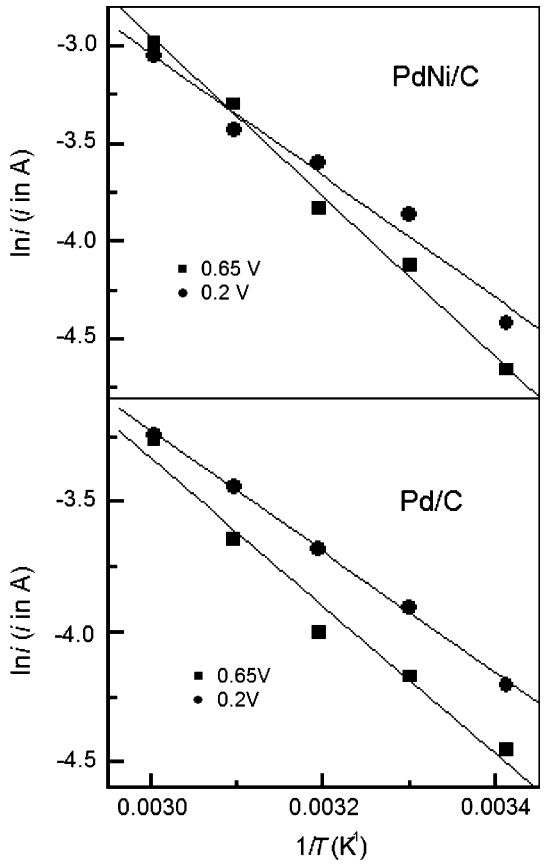

Fig. 7 Arrhenius plots of log *i* versus 1/*T* at 0.2 and 0.65 V for the oxidation of formic acid on Pd/C and PdNi/C electrodes

Table 2 The activation energy for formic oxidation at Pd/C and PdNi/C catalyst electrodes and the standard deviation of the linear fit

Catalyst	Potential (V) (vs. Ag/AgCl)	Activation energy (kJ mol^{-1})	Standard deviation of the linear fit
Pd/C	0.2	19.3	0.056
	0.65	23.5	0.090
PdNi/C	0.2	25.7	0.095
	0.65	33.2	0.067

Figure 7 displays the Arrhenius plots for the current densities of formic acid oxidation reaction at various potentials. Linear relationships exist between log *i* and 1/*T*, indicating that the reaction mechanism at each potential does not change with temperature. The apparent activation energies and the related standard deviation of the linear fit are listed in Table 2. The values of the standard deviation of the linear fit are lower than 0.1, which means that the results have a good linear relationship between log *i* and 1/T. Therefore, the activation energy calculated from the slope of the line is credible. The activation energies on PdNi/C were higher than on Pd/C at the same potential. This means that the activity of formic acid oxidation on PdNi/C was more sensitive to temperature than on Pd/C at both 0.2 and 0.65 V. The increased activation energies with increasing potential mean that the activity of formic acid oxidation was more sensitive to temperature at higher potentials.

Figure 8 shows the chronoamperometry curves of HCOOH in H_2SO_4 solution at Pd/C and PdNi/C catalyst electrodes at 0.2 V. Initially, the current densities rapidly decrease with the time at both electrodes. Subsequently,

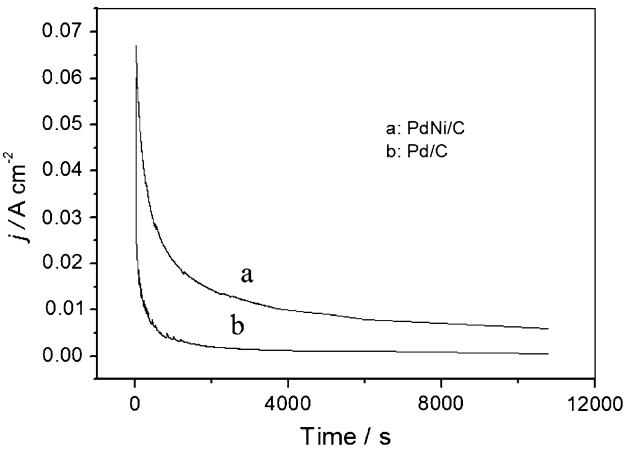

Fig. 8 Chronoamperometric curves of 1.0 M HCOOH in 0.5 M H_2SO_4 at the Pd/C and PdNi/C electrodes at 0.2 V (vs. Ag/AgCl), 25 °C

the current densities decrease slowly and reach a pseudo-steady state. The current density of formic acid oxidation at PdNi/C catalyst electrode is larger than that at Pd/C catalyst electrode at any time within 3 h, illustrating that the electrocatalytic activity and stability of PdNi/C catalyst for formic acid oxidation are better than that of Pd/C catalyst.

4 Conclusions

In the present study, a new carbon-supported PdNi catalyst was prepared by a simple simultaneous reduction reaction with sodium borohydride in glycol solution. It was found that the electrocatalytic activity and stability of PdNi/C catalyst for formic acid oxidation are much better than that of Pd/C catalyst, indicating that Ni can promote the formic acid oxidation reaction at the Pd/C catalyst. Ni exists in the catalyst both as NiO and PdNi alloy. The Pd particles in PdNi/C and Pd/C catalysts were highly dispersed. The activation energy of formic acid oxidation reaction increases with increasing potential. The values of the apparent activation energy show that the electrocatalytic activity of PdNi/C catalyst for formic acid oxidation is more sensitive to temperature compared with that of Pd/C catalyst.

Acknowledgments The authors are grateful for the financial support of The National Natural Science Foundation of China (20573029, 50902041), Natural Science Foundation of Heilongjiang Province (B200905) of China, the Fund of Department of Education of Heilongjiang Province (No. 11531235) of China and The Youth Fund of Harbin Science and Technology Bureau (2007RFQXG059).

References

1. Uhm S, Lee HJ, Kwon Y, Lee J (2008) Angew Chem Int Ed 47:10163
2. Zhang ZH, Huang YJ, Ge JJ, Liu CP, Lu TH, Xing W (2008) Electrochem Commun 10:1113
3. Pan YH, Zhang RM, Blair SL (2009) Electrochem Solid State 12:B23
4. Wang YJ, Wu XC, Wu B, Gao Y (2009) J Power Sources 189:1020
5. Cheng TT, Gyenge EL (2009) J Appl Electrochem 39:1925
6. Vidal-Iglesias FJ, Solla-Gullon J, Herrero E, Aldaz A, Feliu JM (2006) J Appl Electrochem 36:1207
7. Ha S, Dunbar Z, Masel RI (2006) J Power Sources 158:129
8. Zhu YM, Khan Z, Masel RI (2005) J Power Sources 139:15
9. Rhee YW, Ha SY, Masel RI (2003) J Power Sources 117:35
10. Bath BD, White HS, Scott ER (2000) Anal Chem 72:433
11. Rice C, Ha S, Masel RI, Wieckowski A (2003) J Power Sources 115:229
12. Jovanovic VM, Tripkovic D, Tripkovic A, Kowal A, Stoch J (2005) Electrochem Commun 7:1039
13. Chen W, Kim JM, Sun SH, Chen SW (2007) Langmuir 23:11303
14. Tripkovic AV, Popovic KDJ, Lovic JD (2003) J Serb Chem Soc 68:849
15. Choi JH, Park KW, Park IS, Kim K, Lee JS, Sung YE (2006) J Electrochem Soc 153:A1812
16. Chen YX, Heinen M, Jusys Z, Behm RJ (2007) ChemPhysChem 8:380
17. Yu XW, Pickup PG (2009) J Power Sources 187:493
18. Huang YJ, Liao JH, Liu CP, Lu TH, Xing W (2009) Nanotechnology 20
19. Zhou WJ, Lee JY (2008) J Phys Chem C 112:3789
20. Liu ZL, Hong L, Tham MP, Lim TH, Jiang HX (2006) J Power Sources 161:831
21. Jung WS, Han JH, Ha S (2007) J Power Sources 173:53
22. He QG, Chen W, Mukerjee S, Chen SW, Laufek F (2009) J Power Sources 187:298
23. Liu B, Li HY, Die L, Zhang XH, Fan Z, Chen JH (2009) J Power Sources 186:62
24. Wang X, Tang Y, Gao Y, Lu TH (2008) J Power Sources 175:784
25. Yu XW, Pickup PG (2009) J Power Sources 192:279
26. Zhang ZH, Ge JJ, Ma LA, Liao JH, Lu TH, Xing W (2009) Fuel Cells 9:114
27. Wang XM, Xia YY (2008) Electrochem Commun 10:1644
28. Jung CH, Sanchez-Sanchez CM, Lin CL, Rodriguez-Lopez J, Bard AJ (2009) Anal Chem 81:7003
29. Wang JY, Kang YY, Yang H, Cai WB (2009) J Phys Chem C 113:8366
30. Liu ZL, Zhang XH, Hong L (2009) Electrochem Commun 11:925
31. Park KW, Choi JH, Sung YE (2003) J Phys Chem B 107:5851